

Raman microscopy for dynamic molecular imaging of living cells

Keisaku Hamada

Osaka University
Department of Frontier Biosciences
1-3 Yamadaoka, Suita
Osaka 565-0871, Japan

Katsumasa Fujita

Osaka University
Department of Applied Physics
2-1 Yamadaoka, Suita
Osaka 565-0871, Japan
and
RIKEN
Nanophotonics Laboratory
Hirosawa, Wako
Saitama 351-0198, Japan

Nicholas Isaac Smith

Osaka University
Department of Applied Physics
2-1 Yamadaoka, Suita
Osaka 565-0871, Japan

Minoru Kobayashi

Nanophoton Corporation
A-509, CASI,
Osaka University, 2-1 Yamadaoka, Suita
Osaka 565-0871, Japan

Yasushi Inouye

Osaka University
Department of Frontier Biosciences
1-3 Yamadaoka, Suita
Osaka 565-0871, Japan

Satoshi Kawata

Osaka University
Department of Applied Physics
2-1 Yamadaoka, Suita
Osaka 565-0871, Japan
and
RIKEN
Nanophotonics Laboratory
Hirosawa, Wako
Saitama 351-0198, Japan

1 Introduction

Researchers have long sought to improve optical methods of extracting information from living samples by fluorescence, light scattering, or other noninvasive techniques. Raman scattering can be used to optically investigate the chemical properties of samples due to its ability to detect capability of de-

Abstract. We demonstrate dynamic imaging of molecular distribution in unstained living cells using Raman scattering. By combining slit-scanning detection and optimizing the excitation wavelength, we imaged the dynamic molecular distributions of cytochrome *c*, protein beta sheets, and lipids in unstained HeLa cells with a temporal resolution of 3 minutes. We found that 532-nm excitation can be used to generate strong Raman scattering signals and to suppress autofluorescence that typically obscures Raman signals. With this technique, we reveal time-resolved distributions of cytochrome *c* and other biomolecules in living cells in the process of cytokinesis without the need for fluorescent labels or markers. © 2008 Society of Photo-Optical Instrumentation Engineers. [DOI: 10.1117/1.2952192]

Keywords: Raman microscopy; Raman spectroscopy; confocal microscopy; vibrational imaging; molecular imaging.

Paper 07501 received Dec. 29, 2007; accepted for publication Feb. 9, 2008; published online Jul. 18, 2008.

tecting molecular vibration frequencies that characterize molecular species, structures, and environmental conditions. In combination with optical imaging, Raman scattering can be applied to the direct sensing of biological molecules without requiring preprocessing or fluorescence staining of samples.¹⁻⁶ Although Raman scattering is a powerful tool for analyzing biomolecules, it has rarely been attempted as a contrast mechanism for imaging living specimens due to the

Address all correspondence to: Katsumasa Fujita, Department of Applied Physics, Osaka University, 2-1 Yamadaoka, Suita, Osaka 565-0871, Japan. Tel: 816 6879 7847; Fax: 816 6879 7330; E-mail: fujita@ap.eng.osaka-u.ac.jp

extremely low scattering efficiency. Since typical Raman scattering signals are weak (scattering cross-section $\sim 10^{-30}$ cm²) compared to fluorescence yields (absorption cross-section $\sim 10^{-16}$ cm²), the measurement of Raman spectra usually requires long exposure times, making observations of living specimens difficult.

Here, we extend Raman scattering spectroscopy to enable dynamic imaging of molecular distributions in living cells with high temporal and spatial resolution. We combined a slit-scanning detection technique and optimized the excitation wavelength to image molecular distributions of cytochrome *c*, protein beta sheets, and lipids in unstained living HeLa cells. By investigating the wavelength dependencies of Raman signal yields and background signals, we found that 532-nm-wavelength excitation can be used to generate Raman scattering signals strong enough for imaging and for suppressing the background signals that result from autofluorescence. Additionally, cytochrome *c* exhibits resonant Raman scattering by 532 nm excitation, and we found that *in situ* imaging of cytochrome *c* in living cells can finally be performed using our technique. These results show that the activities of molecules, including exogenous molecules such as in pharmaceutical drugs, can be directly monitored in living cells by Raman scattering to identify cellular functions that conventional fluorescence techniques are incapable of revealing.

2 Raman Spectra of Living HeLa Cells

In order to select the excitation wavelength, we first compared Raman spectra of cultured HeLa cells obtained with different excitation wavelengths. We used the standard laser lines: 488 nm from a semiconductor laser, 514.5 nm from an Ar ion laser, 532 nm from a frequency-doubled Nd:YVO₄ laser, and 633 nm from a HeNe laser. Wavelength choice is a tradeoff; shorter wavelengths provide excellent Raman scattering efficiency and spatial resolution, both of which are inversely proportional to wavelength, while longer wavelengths produce significantly less background autofluorescence signals than shorter wavelengths. We used a 1.2 numerical aperture (NA) objective lens, both for illuminating the cells and collecting the Raman signal, using a spectrophotometer (320PI, Acton) and a cooled CCD camera (PIXIS 400BR, Princeton Instruments).

Figure 1 shows the effect of the excitation wavelength on Raman spectra obtained from cytosol regions in living HeLa cells. For each excitation wavelength, we obtained Raman spectra from 36 different positions in the cytosol of a single cell and averaged them to produce each spectrum in Fig. 1, separated by wavelength with no background removal applied. The laser intensity at the focus was 4 mW/ μ m², and the 36 spectra were obtained in parallel over an exposure time of 20 seconds. In Fig. 1, the Raman spectra obtained with the 488-, 514.5-, and 532-nm excitation wavelengths exhibited much stronger scattering signals than the spectra obtained with the 633-nm wavelength, which was expected due to the wavelength dependence of the scattering efficiency. The measured spectra contain peaks that are known to occur in biological samples, such as the ring breathing of phenylalanine (1000 cm⁻¹), CH₂ deformation (1451 cm⁻¹) and CH₂ stretching mode (2850 cm⁻¹, 2885 cm⁻¹), CH₃ stretching

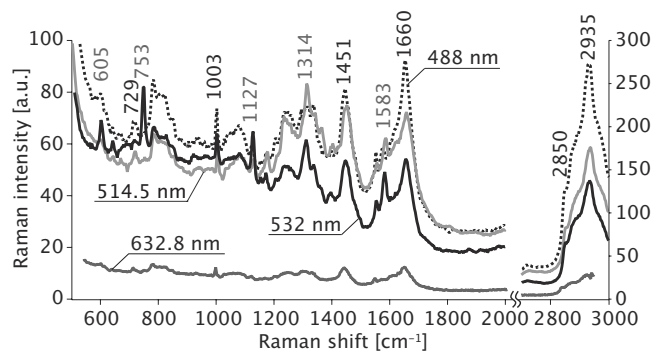


Fig. 1 Raman spectra obtained from the cytosol of a living HeLa cell. Raman spectra obtained from 36 different points in the cytosol of one cell were averaged for each wavelength, showing the tradeoff between Raman peak signal strength and background autofluorescence. The cells were irradiated with laser light of 488-, 514.5-, 532-, and 632.8-nm wavelengths.

mode (2935 cm⁻¹), and Amide-I vibrational mode of peptide bonds (1660 cm⁻¹) (Refs. 7 and 8).

In addition to these typical Raman shifts, strong Raman peaks appear at 753, 1127, 1314, and 1583 cm⁻¹ in the spectra obtained by the 514.5- and 532-nm excitation wavelengths. These peaks can be assigned to vibration modes of cytochrome *c*.⁹ Since cytochrome *c* contains a heme protein that absorbs light at 510 to 550 nm, strong resonant Raman scattering is observed when irradiated with this wavelength range. The Raman peak at 753 cm⁻¹, which shows the pyrrole breathing mode ν_{15} in cytochrome *c*, was previously measured *in vitro* by 532-nm irradiation,⁹ and can be clearly observed *in situ* in this result. By observing the peaks at 753, 1127, 1314, and 1583 cm⁻¹, this technique can be used to detect cytochrome *c* in living cells by resonant Raman scattering. We also measured Raman spectra from the nuclear regions of living HeLa cells (not shown). The Raman spectra from the nuclei were similar, and no substantial spectral dependence on the excitation wavelength was observed, which shows that resonant Raman signals were not a significant contribution to the total Raman emission from the nuclear regions.

We also investigated the contribution of autofluorescence to the background signal in the Raman spectra, which is of particular interest since spectroscopic sensitivity is dramatically reduced by any background contributions due to autofluorescence. The flavin coenzymes FAD and FMN are known to be sources of autofluorescence in the detected wavelength range.^{10,11} Lipofucin is another possible source of autofluorescence; however, it absorbs light predominantly in the UV region and is not significantly excited by the wavelengths used in this experiment.¹² We measured the average fluorescence intensity of FAD at the regions between 600 and 1800 cm⁻¹ for excitation wavelengths of 488, 514.5, and 532 nm. We found that 532-nm excitation produced an autofluorescence signal approximately 12 times lower than 514.5-nm excitation, and 167 times lower than 488-nm excitation. The autofluorescence background signal for 532-nm excitation light was markedly decreased compared to 514.5-nm excitation,

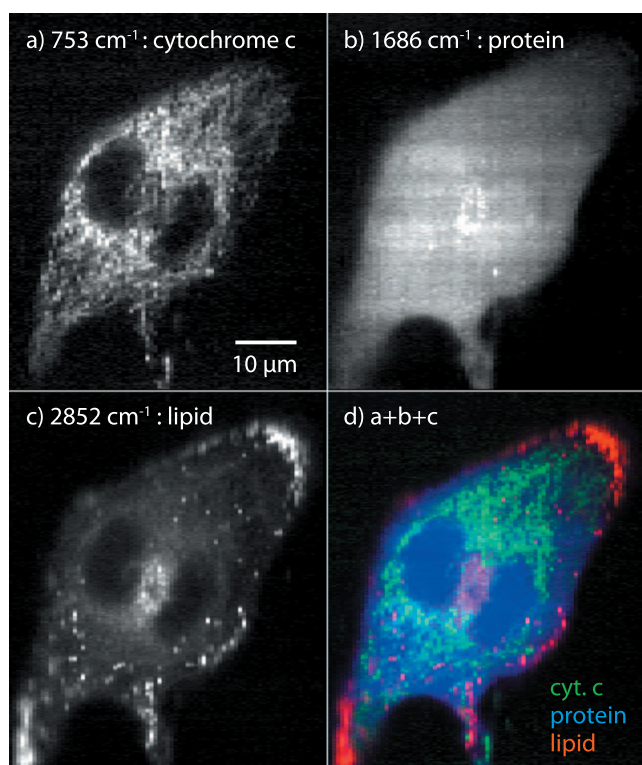
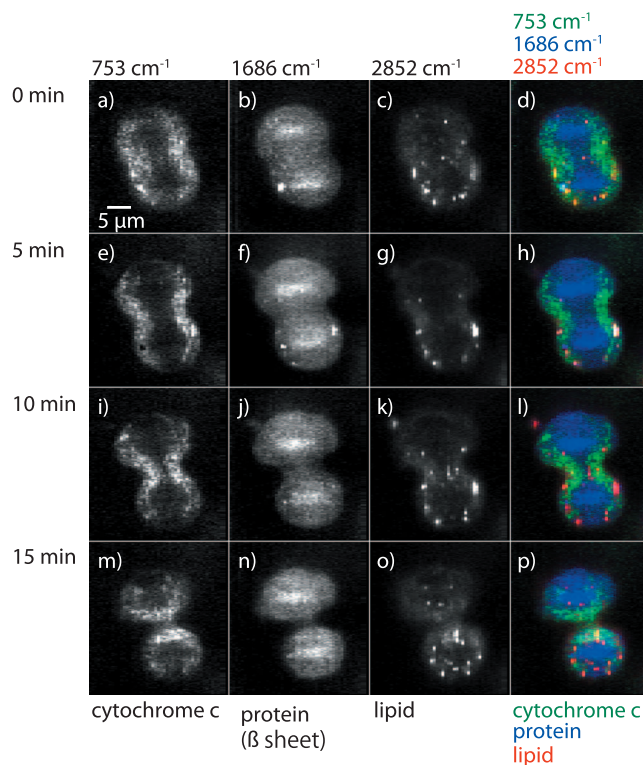


Fig. 2 Raman scattering images of unstained, unlabelled living HeLa cells reconstructed using the distribution of Raman signals at (a) 753 cm^{-1} , (b) 1686 cm^{-1} , and (c) 2852 cm^{-1} , showing the distribution of cytochrome c, protein beta sheet, and lipid molecules, respectively. Image (d) was constructed by merging images (a) through (c) with color channels. The sample was irradiated with a light intensity of $3.3\text{ mW}/\mu\text{m}^2$ at the focal plane in 78 lines of exposure. The exposure time of each line was 5 sec, and the images consist of 78×281 pixels.

and the Raman scattering signals were of comparable strength, which shows that 532-nm excitation is superior for imaging living cell samples.

3 Slit-Scanning Confocal Raman Microscopy

We used a home-made Raman microscope with 532-nm excitation and slit-scanning excitation and detection.^{13,14} The slit-scanning technique allowed us to detect Raman spectra from different positions in parallel, and as a result, greatly improved the image acquisition rate. The sample was irradiated by a line-shaped focus, and Raman scattering signals from the illuminated line were imaged at the entrance slit of a spectrophotometer. Line illumination is also useful in reducing photodamage of the sample because the light intensity at the focal plane is much lower than that of single-focus scanning at the same exposure. Additionally, the slit of the spectrophotometer eliminates Raman scattering from out-of-focus planes, providing spatial resolution in three dimensions and improving of image contrast.¹⁵ To produce the line-shaped laser light, we used a cylindrical lens and imaged the illumination line at the sample by a 1.2-NA water immersion objective lens.



Video 1. Time-resolved imaging of cytochrome c, protein, and lipid molecule distributions in a label-free HeLa cell during cytokinesis. The images were taken at 5-min intervals with a frame rate of 185 sec/image. The progress of cytokinesis is recognized by the change in the distribution of proteins, and a high concentration of cytochrome c is observed at positions near the contractile ring. The sample was irradiated with light intensity of $3.5\text{ mW}/\mu\text{m}^2$ at the focal plane, and the images consist of 161×48 pixel (MOV, 562KB). [URL: <http://dx.doi.org/10.1117/1.2952192.1>].

4 Raman Scattering Images of an Unstained Living HeLa Cell

Using our slit-scanning Raman microscope, we obtained a hyperspectral image of living HeLa cells in the range of Raman shifts between 500 cm^{-1} and 3000 cm^{-1} . The cell was observed in a HEPES-buffered Tyrode's solution composed of (in mM) NaCl, 150; glucose, 10; HEPES, 10; KCl, 4.0; MgCl_2 , 1.0; CaCl_2 , 1.0; and NaOH, 4.0. Then the cell was irradiated with a light intensity of $3.3\text{ mW}/\mu\text{m}^2$ at the focal plane. Singular value decomposition (SVD) was used for noise reduction, and we chose seven loading vectors that significantly contribute to the image contrast for the image reconstruction.⁴ Following noise reduction, we subtracted the fluorescence background signal from the Raman spectra at each pixel in the image by a modified polyfit fluorescence removal technique.¹⁶

The distribution of cytochrome c is reconstructed in Fig. 2(a) from the intensity distribution of the Raman peak at 753 cm^{-1} . Since cytochrome c is used for electron transfer in oxidative phosphorylation in mitochondria, the image has a contrast similar to the distribution of mitochondria. Figure 2(b) shows the Raman signal distribution at 1686 cm^{-1} given by the Amide-I vibration mode of peptide bonds in protein beta sheets.⁷ We chose this wave number because the C-C stretching vibration modes (1650 to 1670 cm^{-1}) in hydrocar-

bon chains of lipid molecules overlap the shorter Raman shifts of the Amide-I band. Since beta sheets are commonly seen in proteins, Fig. 2(b) is strongly correlated with protein distribution in the cell, and consequently, there is a slightly higher protein concentration at the nucleus. Figure 2(c) shows the Raman signal distribution at 2852 cm^{-1} where the signal due to the CH_2 stretching vibration is strongly detected from the hydrocarbon chain of lipid molecules. Although proteins and other biological molecules also contain CH_2 , the image contrast is provided mainly by the lipid vesicles that are rich in lipid molecules.¹⁷ By combining these images via the different color channels of a single image, we obtained the distributions of protein beta sheets, cytochrome c, and lipid vesicles shown in Fig. 2(d).

5 Raman Observation of Dynamic Distributions of Biomolecules

Time-resolved, dynamic molecular distributions are shown in Video 1, where Raman images of a living HeLa cell were taken during cytokinesis. The image acquisition time for each Raman image was 185 seconds, with an interval between images of 115 seconds. The images in Video 1 were obtained with 48 line exposures of 1 second each, for a total exposure time of 48 seconds. The difference between the image acquisition time and the exposure time is due to the data transfer time from the CCD camera to the data storage computer. For Video 1, we also applied noise reduction by the use of SVD, and the images were reconstructed using five loading vectors. The contrast due to Raman scattering in Video 1 indicates that proteins exist in relatively higher concentrations at the chromosomes than in other parts of in the cells, which allows us to trace the progress of cytokinesis by the temporal variation of protein distribution. We also observe that highly concentrated cytochrome c appeared near the cleavage furrow, presumably to provide sufficient energy to the contractile ring that divides the cell into two. In addition, the movement of lipid vesicles associated with cellular dynamics during mitosis can be discerned. During extended observation, photodamage of the cell is a possibility; however, our results show that any photodamage which may have occurred was not significant enough to stop cytokinesis from proceeding.

6 Conclusions

Using the Raman microscopy method described here, we demonstrated label-free observation of biological molecules in living cells using Raman scattering for a contrast mechanism. Label-free imaging provides us with opportunities to observe biological activities without the disturbances of labeling procedures and agents that usually degrade the viability of samples. It frees us from the photobleaching problems inherent in fluorescence staining techniques and allows us to obtain distributions of chemicals in samples that are impossible to stain or in locations where staining is undesirable. We also showed that the resonant Raman scattering of cytochrome c can be distinctly observed using a 532-nm wavelength for excitation, allowing label-free observation of cytochrome c distributed in living cells. Cytochrome c is a protein well known for its important role in the production of ATP in

mitochondria, and the distribution of cytochrome c is thought to change drastically during apoptosis.^{18,19} The Raman imaging technique demonstrated in this paper will allow *in situ* studies of the role of cytochrome c in apoptosis as well as its function in other cellular activities.

References

- G. J. Puppels, F. F. M. de Mul, C. Otto, J. Greve, M. Robert-Nicoud, D. J. Arndt-Jovin, and T. M. Jovin, "Studying single living cells and chromosomes by confocal Raman microspectroscopy," *Nature (London)* **347**, 301–303 (1990).
- G. J. Puppels, M. Grond, and J. Grave, "Direct imaging Raman microscope based on tunable wavelength excitation and narrow-band emission detection," *Appl. Spectrosc.* **47**, 1256–1267 (1993).
- N. Uzunbajakava and C. Otto, "Combined Raman and continuous-wave-excited two-photon fluorescence cell imaging," *Opt. Lett.* **28**, 2073–2075 (2003).
- H.-J. Manen, Y. M. Kraan, D. Roos, and C. Otto, "Intracellular chemical imaging of heme-containing enzymes involved in innate immunity using resonance Raman microscopy," *J. Phys. Chem. B* **108**, 18762–18771 (2004).
- Y.-S. Huang, T. Karashima, M. Yamamoto, and H. Hamaguchi, "Molecular-level investigation of the structure, transformation, and bioactivity of single living fission yeast cells by time- and space-resolved Raman spectroscopy," *Biochemistry* **44**, 10009–10019 (2005).
- J.-X. Cheng and X. S. Xie, "Coherent anti-Stokes Raman scattering microscopy: instrumentation, theory, and applications," *J. Phys. Chem. B* **108**, 827–840 (2004).
- A. T. Tu, *Raman Spectroscopy in Biology: Principles and Applications*, John Wiley & Sons Inc., New York (1982).
- I. Nottingher and L. Hench, "Raman microspectroscopy: a noninvasive tool for studies of individual living cells in vitro," *Expet. Rev. Med. Dev.* **3**, 215–234 (2006).
- T. G. Spiro and T. C. Streckas, "Resonance Raman spectra of hemoglobin and cytochrome c: inverse polarization and vibronic scattering," *Proc. Natl. Acad. Sci. U.S.A.* **69**, 2622–2626 (1972).
- D. L. Heintzelman, R. Lotan, and R. R. Richards-Kortum, "Characterization of the autofluorescence of polymorphonuclear leukocytes, mononuclear leukocytes and cervical epithelial cancer cells for improved spectroscopic discrimination of inflammation from dysplasia," *Photochem. Photobiol.* **71**, 327–332 (2000).
- R. C. Benson, R. A. Meyer, M. E. Zaruba, and G. M. Mckhann, "Cellular autofluorescence—is it due to flavins?" *J. Histochem. Cytochem.* **27**, 44–48 (1979).
- F. Schutt, B. Ueberle, M. Schnolzer, F. G. Holz, and J. Kopitz, "Proteome analysis of lipofuscin in human retinal pigment epithelial cells," *FEBS Lett.* **528**, 217–221 (2002).
- D. K. Veirs, J. W. Ager III, E. T. Loucks, and G. M. Rosenblatt, "Mapping materials properties with Raman spectroscopy utilizing a 2D detector," *Appl. Opt.* **29**, 4969–4980 (1990).
- K. Hamada, K. Fujita, M. Kobayashi, and S. Kawata, "Observation of cell dynamics by laser scanning Raman microscope," *Proc. SPIE* **6443**, 64430Z (2007).
- S. Kawata, R. Arimoto, and O. Nakamura, "Three-dimensional optical-transfer-function analysis for a laser-scan fluorescence microscope with an extended detector," *J. Opt. Soc. Am. A* **8**, 171–175 (1991).
- C. A. Lieber and A. Mahadevan-Jansen, "Automated method for subtraction of fluorescence from biological Raman spectra," *Appl. Spectrosc.* **57**, 1363–1367 (2003).
- J.-X. Cheng, A. Volkmer, L. D. Book, and X. S. Xie, "Multiplex coherent anti-Stokes Raman scattering microspectroscopy and study of lipid vesicles," *J. Phys. Chem. B* **106**, 8493–8498 (2002).
- J. Yang, X. Liu, K. Bhalla, C. N. Kim, A. M. Ibrado, J. Cai, T. Peng, D. P. Jones, and X. Wang, "Prevention of apoptosis by Bcl-2: release of cytochrome c from mitochondria blocked," *Science* **275**, 1129–1132 (1997).
- R. M. Kluck, E. Bossy-Wetzels, D. R. Green, and D. D. Newmeyer, "The release of cytochrome c from mitochondria: a primary site for Bcl-2 regulation of apoptosis," *Science* **275**, 1132–1136 (1997).